

# Effects of annealing and deposition temperature on the structural and optical properties of AZO thin films

I. Kars Durukan · Y. Özen · K. Kizilkaya ·  
M. K. Öztürk · T. Memmedli · S. Özçelik

Received: 24 July 2012 / Accepted: 24 October 2012 / Published online: 4 November 2012  
© Springer Science+Business Media New York 2012

**Abstract** Al-doped ZnO (AZO) thin films were deposited on p-type Si(100) substrate by r.f magnetron sputtering at 200, 300 and 400 °C substrate temperatures. The deposited films were annealed in air atmosphere for 1 h at temperatures of 700, 800 and 900 °C. The deposition temperature and post-deposition annealing effects on structural and optical properties of the AZO samples were analyzed using X-ray diffraction, atomic force microscope and photoluminescence (PL). After annealing, the value of full width half maximum of the diffraction peaks was decreased as well as, the intensity of visible and strong UV PL emission peaks were increased with temperature. However, the deep-level emission related with zinc point defects was removed by annealing of the samples. Results revealed that all of the as-deposited and annealed AZO films have hexagonal structure along (002) direction and their crystallinity were improved with the increased deposition and post-growth annealing temperatures. In addition, the surface roughness and the particle size of the films were increased with increased deposition and annealing temperatures.

## 1 Introduction

Zinc oxide (ZnO) is a preferred material because of its features, such as direct wide band gap ( $\sim 3.4$  eV at the room temperature), large exciton binding energy (60 meV), good piezoelectric properties, high transmittance and high electro-optic coefficient [1–3]. Due to these properties, ZnO is widely used for several industrial applications, such as gas sensors, chemical sensor, piezoelectric devices, nanowires, acoustic wave devices, electric transducers, displays, optical wave guides and solar cells applications [4–6]. ZnO films can be produced in many methods, such as chemical vapor deposition, pulsed laser deposition, e-beam evaporation and magnetron sputtering techniques [7–10]. The sputtering technique is a preferred method for obtaining oxide based low dimensional materials on the variety substrates because of its reproducibility, low cost and low deposition temperature. This technique is also widely used for mass production in industrial application.

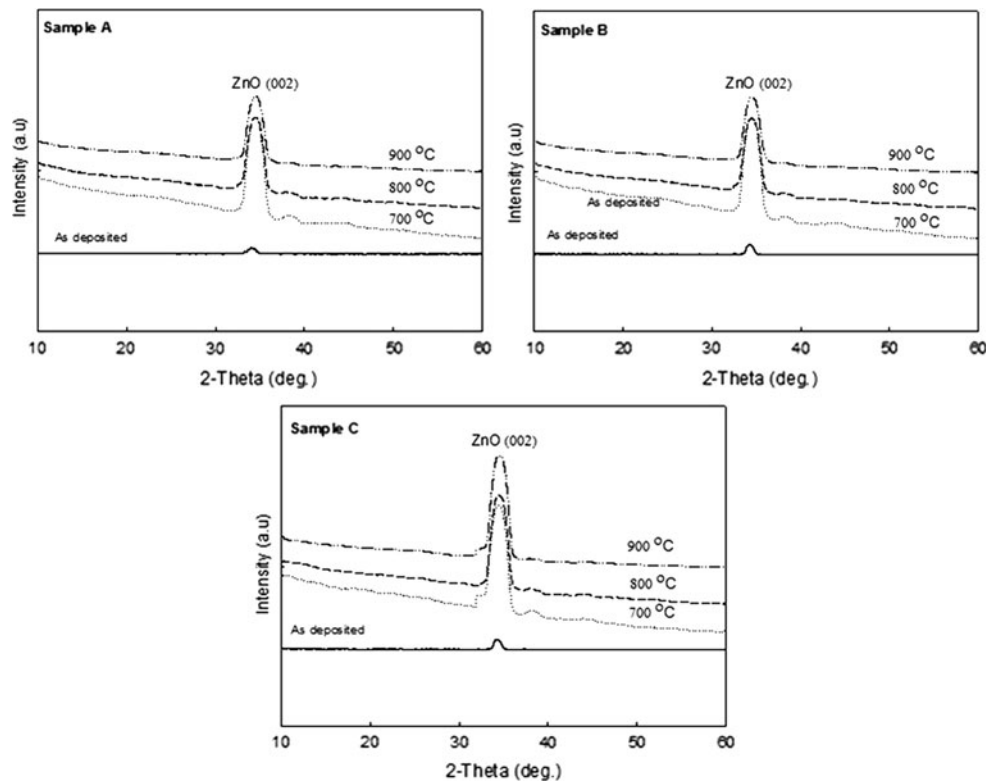
The electro-optical properties of the ZnO films can be improved by doping III-V elements, such as Al, B, Ga and In. In addition, deposition temperature and post-deposition thermally annealing are affect on the crystallinity, surface morphology and photoluminescence (PL) emission of the films. PL spectra of ZnO have ultraviolet (UV) and visible (green-yellow-blue) emission. The UV emission is referred to the near-band-emission (NBE) exciton combination and the visible emission is attributed to transition between defects levels within the bandgap region of the structure [11, 12]. Recently, Deep Level Emission (DLE) have been experimentally studied, and the different interpretations have been given by several researches [13, 14]. However, the origins of different defect emissions are still not fully understood and also, how to change the annealing of defects is still controversial. So, the different defects

---

I. Kars Durukan (✉) · Y. Özen · K. Kizilkaya ·  
M. K. Öztürk · T. Memmedli · S. Özçelik  
Department of Physics, Faculty of Science, Gazi University,  
06500 Ankara, Turkey  
e-mail: ilknurdurukan@gazi.edu.tr

I. Kars Durukan · Y. Özen · K. Kizilkaya ·  
M. K. Öztürk · T. Memmedli · S. Özçelik  
Photonics Research Center, Gazi University, 06500 Ankara,  
Turkey

**Fig. 1** XRD pattern of sample deposited at different substrate temperatures **a** sample A (200 °C), **b** sample B (300 °C) ve **c** sample C (400 °C)



emission in the films must be investigated in detail. Obtained results can provide useful information related with the defect evolution which is very important for the best quality optoelectronic and other optical devices based on AZO films.

In this work, Al doped ZnO (AZO) thin films were deposited on p-type Si (100) substrate by r.f. magnetron sputtering at various substrate temperatures. The films were annealed in air ambience at different temperature. The effects of the deposition temperature and post-deposition annealing temperature on the crystal quality, grain size and

surface morphology of the films were systematically evaluated. In addition, NBE and deep level emission (DLE) of the samples were investigated.

### 2 Experimental

Thickness of 100 nm AZO thin films were grown on p- type Si (100) substrates by rf magnetron sputtering using 4 inch of diameter ZnO with 2 wt% Al<sub>2</sub>O<sub>3</sub> target. The films were deposited at the temperature of 200 , 300 and 400 °C

**Table 1** Structural parameters of AZO thin films obtained by variation of deposition and annealed temperature

Sample (deposition temperature)	Annealing temperature	Orientation	2θ (°)	FWHM(°)	Particle size (nm) with XRD	Grain size(nm) with AFM	Surface roughness (nm)
A (200 °C)	As deposited	(002)	34.153	1.198	6.937	100-200	0.187
	700 °C	(002)	34.539	0.953	8.729	125-335	0.370
	800 °C	(002)	34.511	0.946	8.793	75-500	2.152
	900 °C	(002)	34.574	0.936	8.889	125-1,650	8.705
B (300 °C)	As deposited	(002)	34.344	0.950	8.752	100-230	0.510
	700 °C	(002)	34.538	0.941	8.840	300-600	0.478
	800 °C	(002)	34.602	0.936	8.889	375-850	0.476
	900 °C	(002)	34.667	0.927	8.977	170-2,580	12.932
C (400 °C)	As deposited	(002)	34.336	0.947	8.780	100-200	0.566
	700 °C	(002)	34.606	0.931	8.964	280-480	0.697
	800 °C	(002)	34.528	0.928	8.937	95-650	1.919
	900 °C	(002)	34.602	0.922	9.024	85-750	5.021

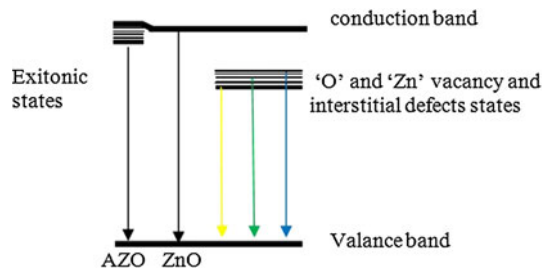


**Fig. 2** Energy transition mechanism from excitonic and the defect states in Al-doped ZnO film

and then were named as A, B and C, respectively. During the deposition, sputtering pressure was kept  $\sim 4 \times 10^{-3}$  mbar and thickness of the films was controlled by a thickness-meter. After the deposition, the thickness of the films was measured with a stylus type profile meter (Veeco-Dektak 150). Sputtering power was fixed at 300 W. In addition, as deposited films were annealed at 700, 800 and 900 °C for 1 h in conventional thermal annealing (CTA) in air atmosphere. Crystal structure and crystallinity of AZO thin films were analyzed by D8-Advance X-ray diffractometer with Cu source ( $\lambda = 1.5406 \text{ \AA}$ ). PL measurement was performed

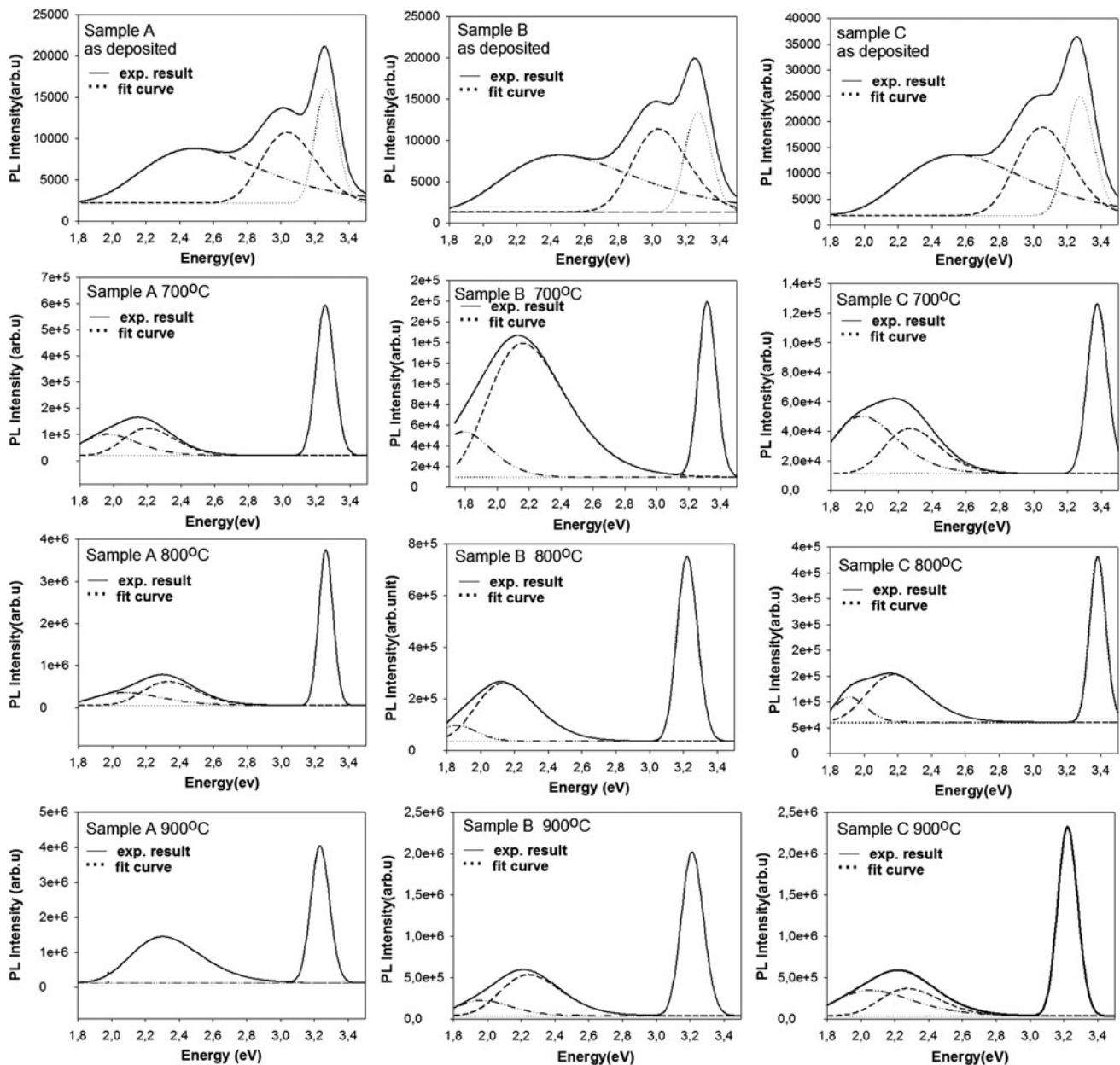


**Fig. 3** PL intensity versus energy of the ZnO films at different annealing temperatures

**Table 2** PL fit results, FWHM and intensity values

Sample	Annealing temperature	Peak-I		Peak-II		Peak-III	
		FWHM	Intensity	FWHM	Intensity	FWHM	Intensity
A (200 °C)	As deposited	15.34	15,897	43.18	10,824	140.62	8,841
	700	12.62	595,286	77.43	124,076	105.77	99,379
	800	9.81	3,766,300	73.11	626,588	114.06	36,850
	900	12.95	4,061,530	94.82	1,429,580		
B (300 °C)	As deposited	17.78	13,251	44.14	11,339	158.13	8,326
	700	14.37	179,509	126.52	138,922	123.12	53,062
	800	12.68	755,744	97.06	256,957	77.04	94,834
	900	15.49	2,015,950	87.47	524,273	99.61	230,031
C (400 °C)	As deposited	18.96	24,499	43.54	18,854	137.08	13,434
	700	12.87	126,051	77.59	41,292	117.85	49,511
	800	10.36	379,622	90.27	153,966	62.40	109,088
	900	13.98	2,324,300	83.30	376,799	130.71	347,869

with Jobin–Yvon Florong-550 PL system with a 50-mW He–Cd laser ( $\lambda = 325$  nm) at room temperature. The surface morphologies and roughness were measured by using an atomic force microscopy (Omicron AFM/STM combine system).

### 3 Result and discussion

Figure 1 shows the XRD patterns of as-deposited at temperature of 200 °C (sample A), 300 °C (sample B), and 400 °C (sample C), and annealed AZO films for 1 h at temperatures of 700, 800 and 900 °C. All of as-deposited and annealed AZO films have a strong X-ray diffraction peak at 34.4° at the (002) plane of the hexagonal phase of the film as seen in Fig. 1. The full-width at half-maximum (FWHM) of (002) diffraction peaks were calculated and their values were tabulated in Table 1. It was observed that the peak intensity increases with deposition temperature. After annealing, there is no significant change in the peak position, however the intensity of (002) peaks was increased and FWHM of the peaks for all grown AZO samples were decreased. These results show that the crystal quality of the films was improved by the increasing of the deposition and annealing temperature.

In addition, the particle size of the films was affected by the deposition and annealing temperatures. The average particle size of the samples was calculated by using Scherrer’s equation [15]:

$$D = \frac{0.9\lambda}{B \cos(\theta)}$$

where  $\lambda$  is the X-ray wavelength of 1.54 Å,  $\theta$  is Bragg diffraction angle, and B is the FWHM of the diffraction peak. Calculated particle size and their values were given in Table 1. Particle size was increased with deposition temperature and also annealing temperature. The sample (sample C) deposited at the highest temperature has bigger particle size than the others at the all annealing temperatures. This results indicate that high deposition temperature contribute to settle the atoms to their lattice site [16, 17]. In addition, both decreasing of FWHM and increasing of the grain size revealed that the crystallinity of the AZO thin films was improved with deposition and annealing temperatures [18, 19].

Figure 3 shows room temperature PL emission spectra of samples A, B and C. The experimental results are shown with solid lines and their Gaussian fits are shown with dashed lines. In PL spectra of as-deposited and annealed AZO films, two kind of emission were observed in UV and

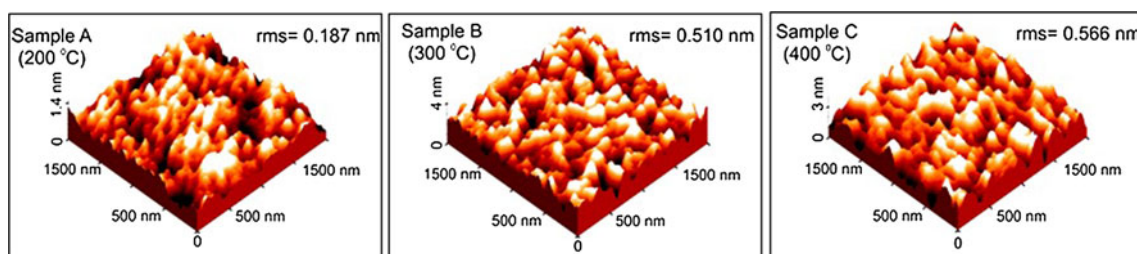


**Fig. 4** AFM surface images ( $2 \mu\text{m} \times 2 \mu\text{m}$ ) of the as-deposited AZO films grown on p-Si substrate at different temperature

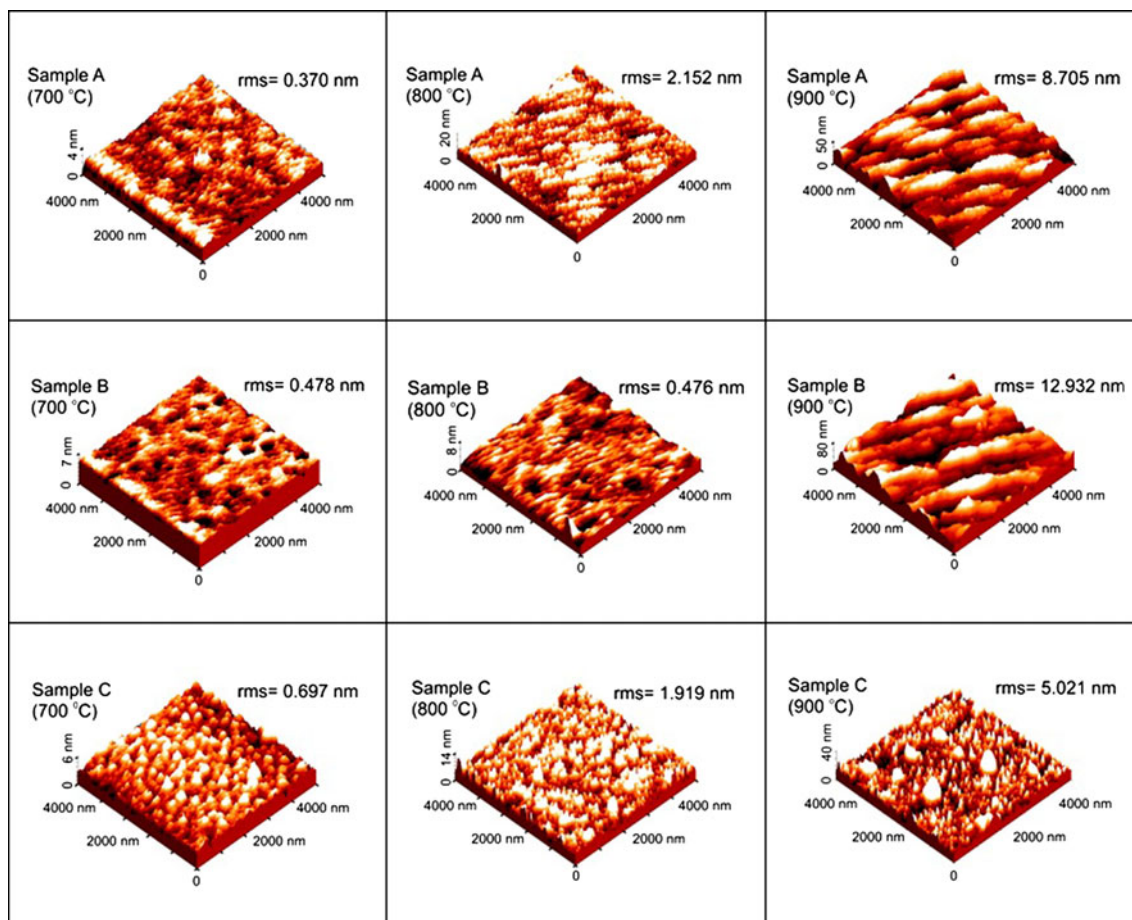


**Fig. 5** AFM images ( $5 \mu\text{m} \times 5 \mu\text{m}$ ) of as annealed at various temperatures from 700 to 900 °C

VIS region: The main emission peak, located at approximately 3.26 eV (380 nm), is attributed to the near band edge emissions (NBE) of the AZO film. This UV emission is derived from recombination of charge carriers produced by photon. The second broad emission peaks correspond to the defect level emission in the band gap region (deep-level transitions), which were observed in the blue-red regions. In case of as-deposited, the defect related two emission peaks around 3.03 eV (408 nm) and 2.54 eV (487 nm) in green–blue wave band were observed. The blue emission located at around 3.03 eV can be attributed to zinc interstitial related defect levels [20]. These emissions are due to transitions from interstitial Zn band to valance band [21]. These kinds of the interstitial defects are observed commonly in zinc rich samples and it is estimated Zn interstitials act as donor centers [22]. The broad emission peak observed around 2.54 eV in green band is known to be a deep level emission which is caused by oxygen vacancy [23]. Moreover, when Al doped in ZnO, oxygen vacancy concentration is high because of site competition between Al and Zn atoms as reported in [24]. Schematic representation of energy transition mechanism from excitonic and

the defect states in Al-doped ZnO film is plotted in Fig. 2. The band gap energy of Al doped ZnO deposited at any temperature is larger than that of undoped ZnO [25].

The values of the intensity and FWHM of the emission peaks of the AZO films were given in Table 2. The intensity of UV emission was increased with annealing temperature. In addition, FWHM values of the UV emission peaks of the samples were decreased with annealing temperature except at 900 °C. Increasing of the values at 900 °C may be explained that the particular crystal size increases in large value and it occurs the oriented mosaic blocs, verifying with X-ray measurement values as shown in Table 1 and AFM images in Fig. 5. When the films were annealed at 700, 800 and 900 °C, the blue emission related with zinc point defects disappeared, however, the intensity of the green emission related with oxygen vacancies increased. This can be explained that the zinc point defects in the samples were decreased as well as the oxygen vacancies concentrations were increased with annealing.

The morphology and the surface roughness of the AZO films determined by AFM measurement are shown Figs. 4 and 5. Three-dimensional (3D) AFM images with  $2 \mu\text{m}^2$



scan area of as-deposited samples are presented in Fig. 4. The surface roughness of the films seems to increase with the increase of substrate temperature, however there is no significant change in grain size. As-deposited samples A, B and C displayed grains in the range of 100–200, 100–230 and 100–200 nm, respectively. Terrace steps and dark spots are randomly located on the thin films surface.

Figure 5 shows three-dimensional (3D) AFM images with  $5 \mu\text{m}^2$  scan area of annealed films. As shown in this figure and Table 1, the surface roughness and the grain size increased with the annealing temperature. However, the surface roughness values of sample B show small fluctuation. The measured size of the grains from AFM surface images is bigger than the particle size calculated from the XRD measurement. The measured size of the grains from AFM and their calculated values from the XRD measurements can not be compared with each other because AFM measurement does not give a direct measure the grain size [26] since the film surface is composed of many clusters of particles [10].

#### 4 Conclusion

AZO thin films were grown at the different substrate temperature of 200, 300 and 400 °C at the same sputtering pressure of  $4.10^{-3}$  mbar. XRD analysis has shown that all films exhibit only the (002) plane of the hexagonal phase. After annealing, any significant change in the peak position was not observed, but (002) peak intensity was enhanced and the full-width at half-maximum (FWHM) for the (002) peaks became narrow. Therefore, increasing annealing temperature improves the quality of the films. In PL spectra of as-deposited and annealed AZO films, two kind of emission were observed. The main emission peak, located approximately at 380 nm (3.26 eV), is attributed to the near band edge emissions (NBE) of the AZO film. The second broad emission peak corresponds to the defect level emission in the band gap region (deep-level transitions) which was observed in the blue-green regions. It is found that luminescence properties of the films changed with an increase of the substrate and annealing temperatures. After annealing, UV emission intensity is increased which is caused by free extion. The blue peak intensity is decreased while the green emission is increased. The concentration of zinc and oxygen defects is changed with the annealed treatment. The surface roughness detected with AFM measurement tends to increase with both an increase of deposition and annealing temperatures, and in the same time particle size becomes larger with the augments of annealing temperature. This is related to the integration of the grains. As a result, the experiments show that the AZO

films deposited at 400 °C has good crystallinity than the others. Also, despite a few structural defects in the films, the optical properties of AZO thin films can be improved with increasing of the annealing temperature.

#### References

1. U. Ozgür, Y.I. Alivov, C. Liu, A. Teke, M.A. Reshchikov, S. Dogan, V. Avrutin, S.-J. Cho, H. Morkoç, J. Appl. Phys. **98**, 041301 (2005)
2. D. Zang, P. Fan, X. Cai, J. Huang, L. Ru, Z. Zeng, G. Liang, Y. Huang, Appl. Phys. A 437–441 (2009)
3. S.-Y. Kuo, W.-C. Chen, F.-I. Lai, C.-P. Cheng, H.-C. Kuo, S.-C. Wang, W.-F. Hsieh, J. Cryst. Growth **287**, 78–84 (2006)
4. D. Zang, P. Fan, X. Cai, J. Huang, L. Ru, Z. Zheng, G. Liang, Y. Huang, Appl. Phys. A **97**, 437–441 (2009)
5. P. Samarasekara, N.U.S. Yapa, N.T.R.N. Kumara, M.V.K. Perera, Bull. Mater. Sci. **30**(2), 113–116 (2007)
6. G. Epurescu, G. Dinescu, A. Moldovan, R. Birjega, F. Dipietrantonio, E. Verona, P. Verardi, L.C. Nistor, C. Ghica, G. Van Tendeloo, M. Dinescu, Superlattices Microstruct. **42**, 79–84 (2007)
7. K.P. Bhuvana, J. Elanchezhian, N. Gopalakrishnan, B.C. Shin, T. Balasubramanian, J. Alloys Compd **478**, 54–58 (2009)
8. C. Wang, Z. Chen, Y. He, L. Li, D. Zang, Appl. Surf. Sci. **255**, 6881–6887 (2009)
9. Q.P. Wang, D.H. Zhang, H.L. Ma, X.H. Zhang, X.J. Zhang, Appl. Surf. Sci. **220**, 12–18 (2003)
10. T. Prasada Rao, M.C. Santhosh Kumar, A. Safarulla, V. Genesan, S.R. Barman, C. Sanjeeviraja, Phys. B **405**, 2226–2231 (2010)
11. R. Baca, G. Juarez, H. Solache, J. Andraca, J. Martinez, A. Asparza, T. Kryshtab, R. Pena, Mater. Sci. Eng **8**, 012041 (2010)
12. B. Cao, W. Cai, H. Zeng, Apply. Phys. Lett **88**, 161101 (2006)
13. A.B. Djuricic, Y.H. Leung, K.H. Tam, Y.F. Hsu, L. Ding, W.K. Ge, Y.C. Zhang, K.S. Wong, W.K. Chan, H.L. Tam, K.W. Cheah, W.M. Kwok, D.L. Phillips, Nanotechnology **18**, 8 (2007)
14. N.H. Alvi, K. ul Hasan, O. Nur, M. Willanger, Nanoscale Res. Lett. **6**, 130 (2011)
15. B.D. Cullity, in *Elements of X-Ray Diffractions*, vol 102. (Addison-Wesley, Reading, 1978)
16. X. Deng, H. Deng, M. Wei, J. Chen, J. Mater. Sci.: Mater. Electron. **23**, 413–417 (2012)
17. S. Wang, X. Liu, J. Zhang, J. Phys: Conf. Ser. **188**, 012017 (2009)
18. W.J. Lee, C.R. Cho, K.M. Cho, S.Y. Jeong, J. Korean Phys. Soc **47**, 296 (2005)
19. W. Yang, Z. Wu, Z. Liu, A. Pang, Y. Tu, Z. Feng, Thin Solid Films **519**, 31–36 (2010)
20. H. Zeng, G. Duan, Y. Li, S. Yang, X. Xu, W. Cai, Adv. Funct. Mater. **20**, 561–572 (2010)
21. Z. Fang, Y. Wang, D. Xu, Y. Tan, X. Liu, Opt. Mater. **26**, 239–242 (2004)
22. D.H. Zhang, Z.Y. Xue, Q.P. Wang, J. Phys. D Appl. Phys. **35**, 2837–2840 (2002)
23. L.M. Li, Z.F. Du, T.H. Wang, Sens. Actuators, B **147**, 165–169 (2010)
24. A. Djelloul, M.-S. Aida, J. Baugdira, J. Lumin. **130**, 2113–2117 (2010)
25. F.K. Shan, Y.S. Yu, J. Eur. Ceram. Soc. **24**, 1869–1872 (2004)
26. S.-K. Wang, T.-C. Lin, S.-R. Jian, J.-Y. Juangb, J.S.C. Jangc, J.-Y. Tsengd, Appl. Surf. Sci. **258**, 1261–1266 (2011)